Biosensors and Bioelectronics 43 (2013) 315–320

Contents lists available at SciVerse ScienceDirect

Biosensors and Bioelectronics

journal homepage: www.elsevier.com/locate/bios

Comparative study on aptamers as recognition elements for antibiotics in a label-free all-polymer biosensor

Johannes Daprà [a], Lasse Holm Lauridsen [b], Alex Toftgaard Nielsen [b], Noemi Rozlosnik [a,*]

[a] Department of Micro- and Nanotechnology, Technical University of Denmark, Produktionstorvet 423, DK-2800 Kgs. Lyngby, Denmark
[b] The Novo Nordisk Foundation Center for Biosustainability, Scion-DTU, Fremtidsvej 3, DK-2970 Hørsholm, Denmark

ARTICLE INFO

Article history:
Received 9 November 2012
Received in revised form
19 December 2012
Accepted 20 December 2012
Available online 7 January 2013

Keywords:
Aptamer
Conductive polymer
Electrochemical impedance spectroscopy
Antibiotics

ABSTRACT

We present an all-polymer electrochemical microfluidic biosensor using Topas® as substrate and a conductive polymer bilayer as electrode material. The conductive bilayer consists of tosylate doped poly(3,4-ethylenedioxythiophene) (PEDOT:TsO) and the hydroxymethyl derivative PEDOT-OH:TsO, which was covalently functionalized with two aptamer probes with affinity to ampicillin or kanamycin A, respectively. Using electrochemical impedance spectroscopy (EIS) we were able to detect ampicillin in a concentration range from 100 pM to 1 μM and kanamycin A from 10 nM to 1 mM. The obtained EIS spectra were fitted with an equivalent circuit model successfully explaining the impedance signal. Real samples from regular ultra-high temperature treated low-fat milk spiked with ampicillin were successfully tested to assess the functionality of the sensor with real samples. In conclusion, we have demonstrated the applicability of the newly developed platform for real time, label-free and selective impedimetric detection of commonly used antibiotics. Additionally it was possible to detect ampicillin in a milk sample at a concentration below the allowed maximum residue limit (MRL) in the European Union.

1. Introduction

Detection, identification and quantification of pathogens and chemical agents are crucial for water and environmental analysis, clinical diagnosis, food safety, and biodefence. The existing immunological or nucleic acid technologies are mostly time consuming and require both sophisticated equipment as well as highly trained personnel, hence increasing the analysis costs. Another limitation of these techniques lies in their nature, which only allows the detection of certain types of analytes.

Therefore, new assay technologies are continuously emerging, and among these, the biosensor technology is the area with fastest growth (Lazcka et al., 2007). Ideally, the assays used in a detection system should enable the detection and quantification of a broad range of different molecules. Furthermore, the technique should provide reliable, real time, on-site, user-friendly, and inexpensive detection with adequate sensitivity, specificity and reproducibility.

Label-free biosensors for in situ measurements with high sensitivity and high specificity are of significant interest for the development of diagnostic devices (Cosnier, 2003; Gerard et al., 2002; Liao et al., 2006).

1.1. Impedimetric biosensors

Impedance spectroscopy is a powerful method to analyse the complex electrical resistance of a system and it is sensitive to surface phenomena and changes of bulk properties. Electrochemical detection using electrochemical impedance spectroscopy (EIS) is advantageous because of its label-free and reagentless character and high sensitivity, as recently reviewed by Pänke et al. (2008). Thus impedance detection is particularly suited to follow binding events in the field of biosensors.

The tools that allow for specific detection (generally referred to as affinity tools) are highly selective binders of the target. At present, antibodies of mammals are the best characterised and most widely used affinity tools, i.e. biological recognition elements in biosensor platforms. However, antibodies do have their limitations: they are sensitive to pH changes and can easily be inactivated (e.g. through elevated temperatures, proteases) (Binz et al., 2005; Hoogenboom, 2005). Moreover, producing antibodies is generally difficult and expensive.

1.2. Aptamers as recognition elements

As alternatives to antibodies, aptamers have recently attracted increasing attention due to their capability to bind a wide range of targets: nucleic acids, proteins, metal ions and other molecules

* Corresponding author. Tel.: +45 27148902.
E-mail addresses: noro58@gmail.com, noro@nanotech.dtu.dk (N. Rozlosnik).

0956-5663/$ - see front matter © 2013 Elsevier B.V. All rights reserved.
http://dx.doi.org/10.1016/j.bios.2012.12.058

with high affinity and sensitivity (Hong et al., 2012; Song et al., 2012b).

Aptamers are peptides or oligonucleotides (RNA or single-stranded DNA; ssDNA) that bind to a specific target molecule. The aptamers typically fold into a three-dimensional structure, whose conformation is changing upon ligand binding. Aptamer-like structures can also be found in nature: riboswitches in bacteria and eukaryotes control translation depending on ligand binding (Winkler et al., 2002).

Novel aptamers can be developed using a process called systematic evolution of ligands by exponential enrichment (SELEX) (Ellington and Szostak, 1990; Tuerk and Gold, 1990). It enables the selection of high-affinity nucleic acid sequences from a random pool of candidates.

The oligonucleotide aptamers can easily be modified with signal moieties and can be produced at low cost. Up to now, a variety of assays have been successfully developed for aptamer-based analysis of biomolecules (Centi et al., 2007; Guo et al., 2008; Wu et al., 2011; Yan et al., 2010).

Efforts have been made to develop aptamer-based biosensors (aptasensors) for sandwich assays in recent years. Although these biosensors could detect the target, the detection limits still need to be improved (Wang et al., 2007; Zuo et al., 2009).

1.3. Detection of antibiotics

The development of novel detection systems for antibiotics is of particular importance. The emergence of microorganisms resistant towards important antibiotics occurs at alarmingly high rates. Infections with multidrug-resistant pathogens have been reported for a range of potentially lethal bacteria including *Staphylococcus aureus* (Klevens et al., 2007) and *Mycobacterium tuberculosis* (Centers for Disease Control and Prevention (CDC), 2006), leaving few or no options for treatment. In the European Union (EU), it is estimated that 25 000 persons die every year from infections with antibiotic-resistant micro-organisms (White et al., 2011). Development of novel antibiotics, however, is attracting little attention from the pharmaceutical industry, and for gram-negative pathogens there are few or no late stage clinical trials of new drugs (Septimus and Kuper, 2009). Besides their use for treating human infections, antibiotics are also utilised as growth promoters in agri- and aquaculture (Cabello, 2006; Witte, 1998).

Due to their short generation time, bacteria can quickly evolve resistance towards all known antibiotics if these are present in sub-lethal concentrations in the environment (Gullberg et al., 2011). To minimise the development of resistance towards antibiotics, it is, therefore, of critical importance to limit both the use and the release of antibiotics into the environment.

Detection of different antibiotics, however, is challenging due to the varied chemical structure of the compounds and the lack of available simple spectroscopic or electrochemical assays.

Recently, aptamers targeting a range of antibiotics, including tobramycin (González-Fernández et al., 2011), kanamycin (Song et al., 2011), ampicillin (Song et al., 2012a) and chloramphenicol (Mehta et al., 2011) have been developed.

1.4. Design of the aptasensor

Polymer-based microfluidic systems meet the requirements of disposable devices for low sample consumption, cost efficiency, reliability, and fast response time, which make the systems ideal for rapid analysis. However, most biosensors for electrochemical detection involve metallic electrodes (Kerman et al., 2004). To avoid oxidation or participation in electrochemical reactions, noble metals such as gold or platinum are usually employed. These materials have a number of disadvantages, such as high (and still increasing) market prices or comparably low biocompatibility. Apart from that they also require very costly fabrication methods.

Conductive polymers offer very suitable properties to master the specialized task of transducing a binding event between an analyte and a biological probe. They have been used as alternative to traditional electrode materials because of the additional advantageous properties of inexpensive electrode fabrication and easy electrode functionalization (Kiilerich-Pedersen et al., 2011; Rozlosnik, 2009).

Because of their excellent compatibility with biological samples, polypyrrole (PPy) and poly(3,4-ethylenedioxythiophene) (PEDOT) have repeatedly been used for sensors in biological environments (Balamurugan and Chen, 2007; Bidan et al., 1999; Dubois et al., 2005; Kiilerich-Pedersen et al., 2011; Sarma et al., 2009; Vidal et al., 1999; Xie et al., 2009).

Even though pyrrole is the less expensive monomer compared to 3,4-ethylenedioxythiophene (EDOT), and PPy shows equally good air stability, PEDOT was used exclusively in this study for its superior stability in phosphate buffers and for its higher conductivity (Groenendaal et al., 2000; Syritski et al., 2005; Yamato et al., 1995).

PEDOT can be processed in different ways. Popular polymerization methods are electropolymerization (Kros et al., 2002; Lima et al., 1998; Shi et al., 2008; Sotzing et al., 1996; Xie et al., 2009; Yamato et al., 1995) or chemical oxidation polymerization in liquid (Aasmundtveit et al., 1999; Hansen et al., 2006, 2007a, 2007b; Winther-Jensen and West, 2006) as well as in vapor phase (Bhattacharyya and Gleason, 2011; Le et al., 2005; Winther-Jensen and West, 2004). Chemical oxidation is advantageous because it does not require a conductive substrate.

Micropatterning of conductive polymers is regularly done using cleanroom-based photolithographic techniques. However, although such processes are versatile, they are not well-suited for fabricating inexpensive biosensor platforms due to their costs. As an alternative, we have recently developed a simple micropatterning procedure, which is based on contacting PEDOT thin films with a micro-structured agarose stamp soaked in a solution of aqueous hypochlorite and a non-ionic detergent (Hansen et al., 2007b; Lind et al., 2012). Where contacted, PEDOT is removed and the underlying substrate exposed. By applying a cyclic-olefin-copolymer (COC) substrate we were able to fabricate nucleotide-functionalized PEDOT microelectrodes on a COC background with a low degree of unspecific binding of DNA, in a simple and inexpensive manner. This sensor has been used to specifically detect picomolar concentrations of antibiotics.

2. Materials and methods

2.1. Chemicals

All chemicals were purchased from Sigma-Aldrich (Schnelldorf, Germany) if not stated otherwise.

2.1.1. Chip material

The substrate and the top part of the microfluidic chip were fabricated from Cyclic Olefin Copolymer (COC) Topas® grade 5013 (T_g at 130 °C, TOPAS Advanced Polymers GmbH, Germany).

2.1.2. Electrode material

For the electrodes, the conducting polymer poly(3,4-ethylene-di-oxy-thio-phene) doped with tosylate (PEDOT:TsO) was used.

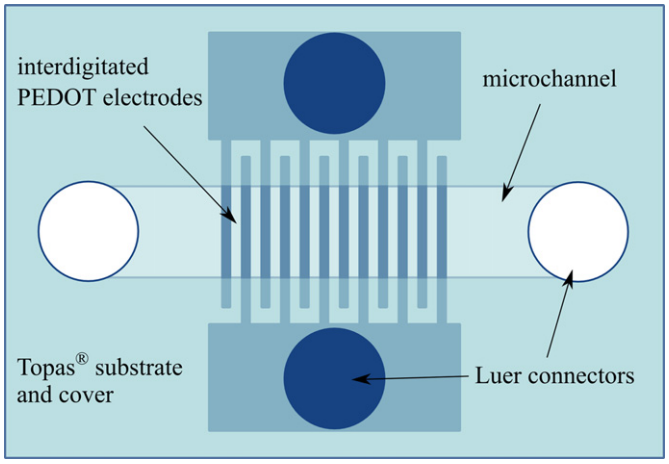

Fig. 1. Schematic drawing of the assembled microfluidic chip with interdigitated PEDOT:TsO electrodes. Drawing is not to scale.

2.1.3. Antibiotics and aptamers

In this study, we used short high-affinity aptamers against kanamycin A and ampicillin presented by Song et al. (2011, 2012a, 2012b), respectively. The DNA aptamers were synthesized by Integrated DNA Technologies (Denmark) as high performance liquid chromatography (HPLC) purified and lyophilized ssDNA functionalized with a 5′-amino modified C_6 linker. Their sequences from 5′ to 3′ are:

Ampicillin	GCG GGC GGT TGT ATA GCG G
Kanamycin A	TGG GGG TTG AGG CTA AGC CGA

2.2. Chip fabrication

The all-polymer microfluidic flow system was fabricated from Topas® polymer using a bilayer composite of PEDOT:TsO and PEDOT-OH:TsO conducting polymer as electrodes (Fig. 1).

Both the top and the bottom part of the chip were made by injection moulding using Topas® pellets.

2.2.1. Conducting polymer film deposition

Conductive thin films of PEDOT:TsO were made by spin coating the reaction solution containing the monomer and thermal activation according to the following procedure:

About 260 µL Baytron C (40% $Fe^{(III)}$ tosylate in butanol), 80 µL butanol, 6 µL pyridine and 8.8 µL EDOT were thoroughly mixed and spun on a 50.8 mm Topas® 5013 disc with 1000 rpm for 60 s. Coated polymer discs were then heated to 70 °C for 5 min. The inhibitor pyridine evaporated and the progress of polymerization was observable by a colour change from yellow to green. After rinsing the discs with de-ionized water to remove excess reactants and by-products, they obtained the characteristic blue colour of PEDOT:TsO. A second polymer layer was applied in the same way using the monomer ((2,3-dihydrothieno[3,4-*b*][1,4]-dioxin-2-yl)methanol) also known as hydroxymethyl-EDOT or EDOT-OH instead of EDOT. This yielded a PEDOT-OH:TsO coating of the same thickness, where the hydroxymethyl group of each monomer provides a possible grafting site for later functionalization.

2.2.2. Microelectrode preparation

Interdigitated microelectrodes were fabricated by agarose stamping, as described in detail by Hansen et al. (2007b) and more recently by Lind et al. (2012).

In short, a stamp was prepared by casting a 10% w/w agarose gel into a mould with a relief of the electrode design etched in silicon. After solidification, the stamp was soaked in the etching solution and applied manually to the PEDOT:TsO/PEDOT-OH:TsO bilayer.

For etching a 1–1.5% w/v solution of sodium hypochlorite in water containing 0.1% v/v of the surfactant TritonX100 was used. The stamping time depends on the thickness of the conductive polymer layer or bilayer, respectively. To etch through approximately 200 nm we needed between 45 and 60 s. After stamping, over-oxidized PEDOT was removed by washing with water. The conducting polymer layers were re-doped by immersion in 4% w/v $Fe^{(III)}$ tosylate solution for a few seconds. During this process, the colour of the polymer changed from dark to light blue indicating the conversion from a reduced state to a more conductive oxidized state with higher degree of doping. The stamp design comprised interdigitated electrodes with a width of 20 µm. The spacing between the single wires was the same as their width.

2.2.3. Chip assembly

The chip consisted of two parts: the flat Topas® disc with the microelectrodes and an injection molded Topas® cover disc with Luer connectors for simple connection to the electronic equipment and exchange of liquids. Both parts were assembled with a 150 µm thick sheet of transfer adhesive (ARcare 90106, Adhesive Research Ireland). Cavities were cut into the tape by laser ablation to create microfluidic channels. To ensure homogeneous and tight sealing around the channels, the assembled discs were pressed with a force of 500 N at a bonding temperature of 75 °C for 5 min. Pressure was released after the chip had cooled down to 40 °C. A schematic drawing of the chip is presented in Fig. 1.

2.2.4. Electrode functionalization

Succinic acid was grafted onto surface hydroxymethyl groups by filling the channels with 0.1 M 2-(*N*-morpholino)ethanesulfonic acid (MES) buffer at pH 4.0 with 50 mM of the coupling agent 1-ethyl-3-(3-dimethylaminopropyl)carbodiimide (EDC) and succinic anhydride for 30 min.

The new surface carboxylic acid groups were activated with 50 mM EDC and 40 mM NHS (*N*-hydroxy succinimide) in MES buffer (0.1 M, pH=4.0) for 5 min. After washing with MES buffer, the 5′-amino modified aptamer (100 nM in MES) was added to form a stable amide bond.

After a reaction time of 3 h, the channels were rinsed with several millilitres of binding buffer (DPBS; Dulbecco's phosphate buffered saline, containing 5 mM $MgCl_2$).

To verify the success of the immobilization, the grafting method was tested with fluorescently labeled DNA. Control experiments without activation reagents showed that no non-specifically adsorbed DNA remained after washing. Fluorescence micrographs are shown in Fig. S1 in the electronic supplementary information.

2.3. Electrochemical impedance measurements

Electrochemical impedance spectroscopy (EIS) was conducted on chips with and without immobilized aptamers. A potentiostat with integrated frequency generator (Zahner IM6, Zahner Elektrik GmbH, Germany) was connected to the electrodes by spring-loaded (Pogo Pin) contacts and the impedance of the system was measured with wide spectrum sweeps in a frequency range from 100 kHz to 200 mHz (logarithmic scale with 10 points per decade for frequencies <66 Hz and four points per decade for frequencies >66 Hz). After the baseline was recorded, the target was

added in increasing concentrations and the change of the impedance signal monitored.

3. Results and discussion

3.1. Film characterization

As has been reported in previous publications, the conductivity of both PEDOT:TsO and PEDOT-OH:TsO is, compared to other conjugated polymers, very high. Surface conductivity values of up to 700 S/cm have been found for PEDOT:TsO (Hansen et al., 2007b; Winther-Jensen and West, 2006), while for tosylate doped hydroxymethyl-PEDOT a value of 83 S/cm has been reported (Hsiao et al., 2010).

Our findings for PEDOT:TsO were 424 ± 57.2 S/cm and for PEDOT-OH:TsO 81 ± 10.7 S/cm. The double layer composite showed a conductance of 275 ± 61.2 S/cm. The conductances of our polymer films are, therefore, within the expected range.

3.2. Micropatterning

After stamping, the actual width of the micro-electrode wires was determined by optical microscopy. Despite being designed with a width of 20 μm, the mean width of the wires was measured to be 9.7 ± 2.2 μm. The large deviation from the original wire size can be explained by diffusion processes occurring during stamping. Shortening the exposure time would certainly reduce the effect; however, then the etching of the desired areas would not be complete, resulting in residual conductivity between the wires. Uniform pressure control by automation of the stamping process would improve the reproducibility significantly.

3.3. Impedimetric characterization of the aptasensor

In this study, we show that the above-described all-polymer biosensor is a sensitive and selective platform for detection of different antibiotics. We have chosen already published aptamers against kanamycin A and ampicillin for our experiments (Song et al., 2011, 2012a).

The immobilization of the aptamers alone provoked an increase in the impedance, as was expected due to the increased charge transfer resistance at the electrode/liquid interface.

Binding of the target molecules to the corresponding aptamer caused a further increase in the impedance measured at frequencies below 1 Hz. A logarithmic correlation of analyte concentration and impedance response was found for a broad dynamic range and both analytes. In the following, the individual aptasensors will be discussed in more detail.

Analyte concentrations starting from 10 pM were tested with ampicillin-aptamer. Fig. 2 shows the relative change of absolute impedance with increasing concentrations. The first statistically significant ($p < 0.05$) signal was observed at 100 pM. Further increase of analyte concentration showed a fairly linear dependence in the logarithmic plot.

As described above, the patterning of the chips was subject to uncertainties, which resulted in variation in the width of the electrodes in the range of several micrometers.

There was a very good correlation between impedance change and wire size (see Fig. S2 in the electronic supplementary information), so that a better reproducibility can be expected from electrodes fabricated with higher accuracy.

With a dissociation constant $k_D = 78.8$ nM the kanamycin A aptamer establishes a weaker bond to its target than the ampicillin aptamer ($k_D = 13.4$ nM) (Song et al., 2011, 2012a). It is, therefore, likely that an aptasensor based on this probe would be less sensitive. As shown in Fig. 2 our findings verify this presumption. Typically a concentration of 10 nM was necessary to obtain a statistically significant increase ($p < 0.05$) of the impedance modulus. Lower concentrations, starting from 10 pM, caused little or no effect on the signal. We believe that the relatively low limit of detection (LOD) and wide dynamic range of the biosensor is also due to specific device properties and not exclusively related to affinity of the probes used in this study. In addition, sensors and assays for Ochratoxin A (OTA) have shown that using the same aptamer in different assays and sensors can result in over a 1000-fold differences in LOD (Lauridsen and Veedu, 2012). The lower detection limit found with the ampicillin aptamer indicates that a high affinity for target compounds will facilitate higher devise sensitivity.

Control experiments, where the antibiotics were reacted with the mismatching aptamers, gave no changes in the impedance signal compared to the baseline. After that, injecting the matching antibiotics into the biosensor resulted in the expected increase of impedance. This shows that the immobilization of the aptamers on the electrodes did not affect the selectivity of the aptamers towards their targets.

With the described experimental setup (see Section 2.3) we were able to obtain one full impedance spectrum in 2:35 min. Fig. 3 shows the impedance data at a single frequency (356 mHz), which was taken from the full spectra. As can be seen in the graph, the impedance change occurs within the sampling time, i.e. within 2:35 min and stabilizes at a new level. We have also conducted impedance measurements at a single frequency, where

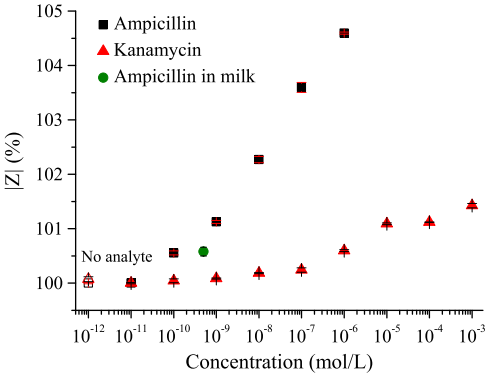

Fig. 2. A typical impedance response for increasing concentrations of ampicillin or kanamycin, respectively. The empty symbols illustrate the measured baseline level before the first injection. The green circle represents the obtained impedance change in the case of 500 mol/L ampicillin in milk sample. The error bars show the average of the signal noise. (For interpretation of the references to color in this figure caption, the reader is referred to the web version of this article.)

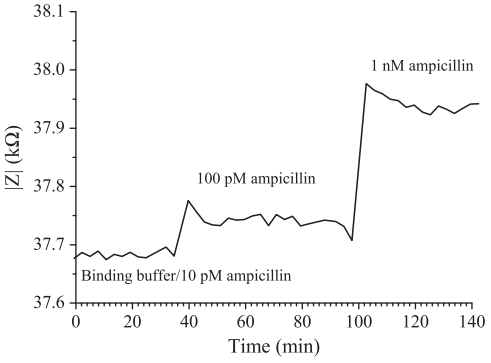

Fig. 3. Increase of impedance at a frequency of 356 mHz is shown after addition of the analyte in different concentrations.

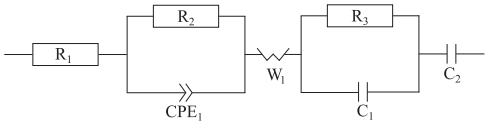

Fig. 4. Equivalent circuit model for fitting the experimental spectra (see description in the text).

the instrument-determined minimum sampling time was ca. 17 s (data not shown), but also this higher temporal resolution was insufficient to determine the reaction rate of the target-aptamer complex formation. However, this shows that the analysis time is reasonably short for a number of real-life applications.

EU regulation no. 675/92 (as amendment to regulation no. 2377/90) lays down a maximum residue limit (MRL) for ampicillin of 4 μg/L in milk, which is equivalent to a concentration of 11.45 nM. Our experiments shown above proved that we were able to detect much lower concentrations of ampicillin in buffer solution. In order to prove the reliability of the sensor detecting analytes in real samples, a 10% solution of ultra-high temperature treated (UHT) low fat milk in DPBS containing 5 mM $MgCl_2$ was prepared and spiked with 500 pM ampicillin. Impedance spectra were measured as before. In these experiments, we were able to measure an increase of impedance of $0.58 \pm 8\%$. These data are in well accordance with the concentration dependence reported above. We can, therefore, claim that our sensor is capable of reproducibly detecting an ampicillin concentration in milk that is far below the MRL set by the EU.

3.4. Equivalent circuit modeling of the EIS results

An equivalent circuit model fitting the electrical properties of the sensor is shown in Fig. 4. This model was used to simulate impedance spectra while changing certain parameters to understand the effects observed in our experiments; it satisfactorily fits the experimental data over the measured frequency range.

In the model, R_1 is the intrinsic resistance of the electrodes. The parallel resistance (R_2) and the constant phase element (CPE_1) with coefficients P_1 and n_1 represent the electrode–solution interface, where R_2 is the charge transfer resistance and CPE_1 the electrical double layer on the surface. The following Warburg impedance (W_1) indicates the diffusion limited electrochemical processes specified by the coefficient A_{w1}. The impedance spectrum includes a semicircle portion at high frequencies corresponding to bulk solution resistance (R_3) and the geometrical capacitance (C_1) of the interdigitated electrodes. Finally, the capacitance C_2 is the limiting capacitance, which reflects the limited solid state diffusion of charges inside the conducting polymer.

The intrinsic resistance of the electrode (R_1), the solution resistance (R_3) and electrode geometrical capacitance (C_1) are not changing during the aptamer-target binding process. The Warburg coefficient (A_{w1}) represents the impedance due to the diffusion of charges to and from the electrode surface. The temperature and the viscosity of the solution were constant during the binding process; however, conformational changes and rearrangements of the surface bound aptamers during complex formation are likely to alter the electrode surface area available for charge transfer, influencing A_{w1}. Modifications of the electrode surface can inflict changes to the electrolytic double layer at the electrode/electrolyte interface with its non-ideal capacitance (reflected as the constant phase element CPE_1) and the reaction rate of the transfer of charges between electrode and electrolyte (expressed as the charge transfer resistance R_2). Both factors are dependent on the change of the ionic concentration near the electrode surface, which is influenced by the binding event of an analyte molecule to an immobilized aptamer. We can, therefore, assume that both the constant phase element, the charge transfer resistance and the Warburg element will be the most interesting parameters for investigations of target binding to surface-bound probes. The surface coverage with aptamers could have an influence on the sensitivity of such a device as described here, but the size of the antibiotics is much less that than the aptamers, therefore, it is not likely that steric hindrance would affect the results.

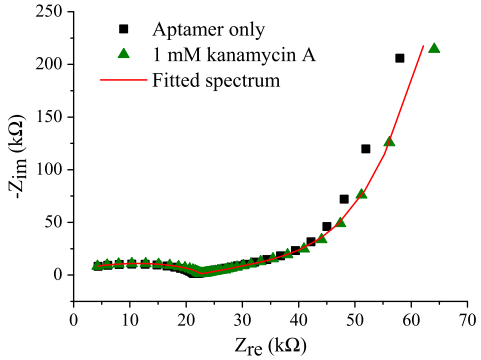

Fig. 5. Nyquist plots from impedance spectra before (■) and after (▲) addition of kanamycin A. In the low frequency region (right side) of the spectra a clear shift towards higher resistance is visible. The solid red line represents a simulated spectrum based on the fitting parameters from Table 1. The curve is calculated from the values after analyte addition. (For interpretation of the references to color in this figure caption, the reader is referred to the web version of this article.)

Table 1
Comparison of parameters corresponding to elements in the equivalent circuit model fitted to the spectra shown in Fig. 5.

Parameter	Aptamer only (error/%)	Kanamycin (error/%)	Unit
C_1	1.59×10^{-10} (2.8)	1.58×10^{-10} (2.3)	F
C_2	4.11×10^{-6} (2.3)	4.06×10^{-6} (3.0)	F
R_1	3.34×10^{2} (41.3)	3.07×10^{2} (46.7)	Ω
R_2	2.51×10^{4} (7.8)	2.41×10^{4} (9.3)	Ω
R_3	2.06×10^{4} (0.8)	2.16×10^{4} (0.8)	Ω
A_{w1}	1.44×10^{4} (12.8)	2.13×10^{4} (9.0)	$\Omega/\sqrt{s}$
P_1	5.75×10^{-6} (6.2)	6.80×10^{-6} (6.9)	$1/\Omega$
n_1	0.58 (1.9)	0.57 (2.2)	–

Impedance spectra recorded at different stages of the experiment were fitted with the "EIS Spectrum Analyser" software.[1] An example of the fitted curves is shown together with two measured spectra represented as a Nyquist plot in Fig. 5. The curve was calculated from parameters which were fitted to the impedance data obtained from the kanamycin aptasensor after the analyte was added. The result indicates a good agreement with the measured data, especially in the lower frequency range.

A comparison of parameters obtained from fitting the model to the data recorded before analyte addition and after injection of kanamycin A at a concentration of 1 mM is made in Table 1. As expected, only slight changes were observed for the capacitances C_1 and C_2 as well as the material or solution related resistances R_1 and R_3. Elements describing the electrode/liquid interface experienced a larger change. The strongest deviation from the original value was found for the Warburg coefficient A_{w1}.

4. Conclusion

We have successfully developed the first prototype of an all-polymer electrochemical biosensor using Topas® as microfluidic

[1] A.S. Bondarenko and G.A. Ragoisha, http://www.abc.chemistry.bsu.by/vi/analyser/.

system and a bilayer of tosylate doped poly(3,4-ethylenedioxythiophene) (PEDOT:TsO) and its hydroxymethyl derivative PEDOT-OH:TsO as electrode material covalently functionalized with aptamers. The newly developed inexpensive biosensor has high sensitivity and selectivity for the tested targets, which makes it a promising platform for detection of analytes from complex samples by a fast, label-free and reliable method. The device was tested with real samples from milk, where it was possible to detect ampicillin in concentrations below the MRL defined in EU regulation no. 675/92.

Acknowledgement

This project was financially supported by funding from the Danish Research Council, The Novo Nordisk Foundation and the Technical University of Denmark.

Appendix A. Supplementary data

Supplementary data associated with this article can be found in the online version at http://dx.doi.org.10.1016/j.bios.2012.12.058.

References

Aasmundtveit, K.E., Samuelsen, E.J., Pettersson, L.A.A., Inganäs, O., Johansson, T., Feidenhans'l, R., 1999. Synthetic Metals 101 (1–3), 561–564.
Balamurugan, A., Chen, S.-M., 2007. Analytica Chimica Acta 596 (1), 92–98.
Bhattacharyya, D., Gleason, K.K., 2011. Chemistry of Materials 23 (10), 2600.
Bidan, G., Billon, M., Livache, T., Mathis, G., Roget, A., Torresrodriguez, L., 1999. Synthetic Metals 102 (1–3), 1363.
Binz, H., Amstutz, P., Plückthun, A., 2005. Nature Biotechnology 23 (10), 1257–1268.
Cabello, F.C., 2006. Environmental Microbiology 8 (7), 1137–1144.
Centers for Disease Control and Prevention (CDC), March 2006. MMWR. Morbidity and Mortality Weekly Report 55(11), 301–305.
Centi, S., Tombelli, S., Minunni, M., Mascini, M., 2007. Analytical Chemistry 79 (4), 1466–1473.
Cosnier, S., 2003. Analytical and Bioanalytical Chemistry 377 (3), 507–520.
Dubois, M.-P., Gondran, C., Renaudet, O., Dumy, P., Driguez, H., Fort, S., Cosnier, S., 2005. Chemical Communications (Cambridge) (34), 4318–4320.
Ellington, A.D., Szostak, J.W., 1990. Nature 346 (6287), 818–822.
Gerard, M., Chaubey, A., Malhotra, B., 2002. Biosensors and Bioelectronics 17 (5), 345–359.
González-Fernández, E., de-los Santos-Álvarez, N., Lobo-Castañón, M.J., Miranda-Ordieres, A.J., Tuñón-Blanco, P., 2011. Biosensors and Bioelectronics 26 (January (5)), 2354–2360.
Groenendaal, L., Jonas, F., Freitag, D., Pielartzik, H., Reynolds, J.R., 2000. Advanced Materials 12 (7), 481.
Gullberg, E., Cao, S., Berg, O.G., Ilbäck, C., Sandegren, L., Hughes, D., Andersson, D.I., 2011. PLoS Pathogens 7 (July (7)).
Guo, W., Yuan, J., Li, B., Du, Y., Ying, E., Wang, E., 2008. Analyst 133 (9), 1209–1213.
Hansen, T.S., West, K., Hassager, O., Larsen, N.B., 2006. Synthetic Metals 156 (18–20), 1203.
Hansen, T.S., West, K., Hassager, O., Larsen, N.B., 2007a. Journal of Micromechanics and Microengineering 17 (5), 860.
Hansen, T.S., West, K., Hassager, O., Larsen, N.B., 2007b. Advanced Materials 19 (20), 3261.
Hong, P., Li, W., Li, J., 2012. Sensors 12 (2), 1181–1193.
Hoogenboom, H., 2005. Nature Biotechnology 23 (9), 1105–1116.
Hsiao, A.-E., Tuan, C.-S., Lu, L.-H., Liao, W.-S., Teng, W.-J., 2010. Synthetic Metals 160 (21–22), 2319.
Kerman, K., Kobayashi, M., Tamiya, E., 2004. Measurement Science and Technology 15 (2).
Kiilerich-Pedersen, K., Poulsen, C.R., Jain, T., Rozlosnik, N., 2011. Biosensors and Bioelectronics, 386–392.
Klevens, R.M., Morrison, M.A., Nadle, J., Petit, S., Gershman, K., Ray, S., Harrison, L.H., Lynfield, R., Dumyati, G., Townes, J.M., Craig, A.S., Zell, E.R., Fosheim, G.E., McDougal, L.K., Carey, R.B., Fridkin, S.K., 2007. JAMA—Journal of the American Medical Association 298 (15), 1763–1771.
Kros, A., Nolte, R.J.M., Sommerdijk, N.A.J.M., 2002. Journal of Polymer Science. Part A—Polymer Chemistry 40 (6), 738.
Lauridsen, L., Veedu, R., 2012. Nucleic Acid Therapeutics. 22 (6), 371–379, http://dx.doi.org/10.1089/nat.2012.0377.
Lazcka, O., Campo, F.J.D., Muñoz, F.X., 2007. Biosensors and Bioelectronics 22 (7), 1205–1217.
Le, T.T., Kim, D.W., Lee, Y., Nam, J.D., 2005. Accessed online 25.11.2010 〈http://gralib.hcmuns.edu.vn/gsdl/collect/hnkhbk/index/assoc/HASH01f3/8a663927.dir/doc.pdf〉.
Liao, W., Guo, S., Zhao, X., 2006. Frontiers in Bioscience 11, 186–197.
Lima, A., Schottland, P., Sadki, S., Chevrot, C., 1998. Synthetic Metals 93 (February (1)), 33–41.
Lind, J.U., Acikgoz, C., Daugaard, A.E., Andresen, T.L., Hvilsted, S., Textor, M., Larsen, N.B., 2012. Langmuir 28 (15), 6502–6511.
Mehta, J., Van Dorst, B., Rouah-Martin, E., Herrebout, W., Scippo, M.-L., Blust, R., Robbens, J., 2011. Journal of Biotechnology 155 (4), 361–369.
Pänke, O., Balkenhohl, T., Kafka, J., Schäfer, D., Lisdat, F., 2008. Biochemical Engineering & Biotechnology 109, 195–237.
Rozlosnik, N., 2009. Analytical and Bioanalytical Chemistry 395 (3), 637–645.
Sarma, A.K., Vatsyayan, P., Goswami, P., Minteer, S.D., 2009. Biosensors and Bioelectronics 24 (8), 2313–2322.
Septimus, E.J., Kuper, K.M., 2009. Clinical Pharmacology & Therapeutics 86 (September (3)), 336–339.
Shi, Y., Luo, S., Fang, W., Zhang, K., Ali, E., Boey, F., Ying, J., Wang, J., Yu, H., Li, L., 2008. Organic Electronics 9 (5), 859.
Song, K.-M., Cho, M., Jo, H., Min, K., Jeon, S.H., Kim, T., Han, M.S., Ku, J.K., Ban, C., 2011. Analytical Biochemistry 415 (2), 175–181.
Song, K.-M., Jeong, E., Jeon, W., Cho, M., Ban, C., 2012a. Analytical and Bioanalytical Chemistry 402 (6), 2153–2161, http://dx.doi.org/10.1007/s00216-011-5662-3.
Song, K.-M., Lee, S., Ban, C., 2012b. Sensors 12 (1), 612–631.
Sotzing, G.A., Reynolds, J.R., Steel, P.J., 1996. Chemistry of Materials 8 (April (4)), 882–889.
Syritski, V., Gyurcsányi, R.E., Öpik, A., Tóth, K., 2005. Synthetic Metals 152 (1–3), 133–136.
Tuerk, C., Gold, L., 1990. Science 249 (4968), 505–510.
Vidal, J.C., Méndez, S., Castillo, J.R., 1999. Analytica Chimica Acta 385 (1–3), 203–211.
Wang, J., Wang, L., Liu, X., Liang, Z., Song, S., Li, W., Li, G., Fan, C., 2007. Advanced Materials 19 (22), 3943–3946.
White, A.R., on behalf of the BSAC Working Party on The Urgent Need: Regenerating Antibacterial Drug Discovery and Development, Blaser, M., Carrs, O., Cassell, G., Fishman, N., Guidos, R., Levy, S., Powers, J., Norrby, R., Tillotson, G., Davies, R., Projan, S., Dawson, M., Monnet, D., Keogh-Brown, M., Hand, K., Garner, S., Findlay, D., Morel, C., Wise, R., Bax, R., Burke, F., Chopra, I., Czaplewski, L., Finch, R., Livermore, D., Piddock, L. J.V., White, T., 2011. Journal of Antimicrobial Chemotherapy 66(9), 1948–1953.
Winkler, W., Nahvi, A., Breaker, R.R., 2002. Nature 419 (October (6910)), 952–956.
Winther-Jensen, B., West, K., 2004. Macromolecules 37 (12), 4538–4543.
Winther-Jensen, B., West, K., 2006. Reactive and Functional Polymers 66 (5), 479–483.
Witte, W., 1998. Science 279 (5353), 996–997.
Wu, S., Duan, N., Wang, Z., Wang, H., 2011. Analyst 136, 2306–2314.
Xie, H., Luo, S.-C., Yu, H.-H., 2009. Small 5 (22), 2611–2617.
Yamato, H., Ohwa, M., Wernet, W., 1995. Journal of Electroanalytical Chemistry 397 (1–2), 163–170.
Yan, X., Cao, Z., Lau, C., Lu, J., 2010. Analyst 135, 2400–2407.
Zuo, X., Xiao, Y., Plaxco, K., 2009. Journal of the American Chemical Society 131 (20), 6944–6945.